

RESEARCH

Open Access



# Proneurogenic actions of follicle-stimulating hormone on neurospheres derived from ovarian cortical cells in vitro

Alfredo González-Gil<sup>1\*</sup>, Belén Sánchez-Maldonado<sup>2</sup>, Concepción Rojo<sup>3</sup>, Miguel Flor-García<sup>4,5</sup>, Felisbina Luisa Queiroga<sup>6,7\*</sup>, Susana Ovalle<sup>8</sup>, Ricardo Ramos-Ruiz<sup>8</sup>, Manuel Fuertes-Recuero<sup>1</sup> and Rosa Ana Picazo<sup>1</sup>

## Abstract

**Background** Neural stem and progenitor cells (NSPCs) from extra-neural origin represent a valuable tool for autologous cell therapy and research in neurogenesis. Identification of proneurogenic biomolecules on NSPCs would improve the success of cell therapies for neurodegenerative diseases. Preliminary data suggested that follicle-stimulating hormone (FSH) might act in this fashion. This study was aimed to elucidate whether FSH promotes development, self-renewal, and is proneurogenic on neurospheres (NS) derived from sheep ovarian cortical cells (OCCs). Two culture strategies were carried out: (a) long-term, 21-days NS culture (control vs. FSH group) with NS morphometric evaluation, gene expression analyses of stemness and lineage markers, and immunolocalization of NSPCs antigens; (b) NS assay to demonstrate FSH actions on self-renewal and differentiation capacity of NS cultured with one of three defined media: M1: positive control with EGF/FGF2; M2: control; and M3: M2 supplemented with FSH.

**Results** In long-term cultures, FSH increased NS diameters with respect to control group ( $302.90 \pm 25.20 \mu\text{m}$  vs.  $183.20 \pm 7.63$  on day 9, respectively), upregulated *nestin* (days 15/21), *Sox2* (day 21) and *Pax6* (days 15/21) and increased the percentages of cells immunolocalizing these proteins. During NS assays, FSH stimulated NSPCs proliferation, and self-renewal, increasing NS diameters during the two expansion periods and the expression of the neuron precursor transcript *DCX* during the second one. In the FSH-group there were more frequent cell-bridges among neighbouring NS.

**Conclusions** FSH is a proneurogenic hormone that promotes OCC-NSPCs self-renewal and NS development. Future studies will be necessary to support the proneurogenic actions of FSH and its potential use in basic and applied research related to cell therapy.

**Keywords** FSH, Neurogenesis, Neurosphere, Neural stem and progenitor cells, Endocrine, Ovarian cortical cells

\*Correspondence:

Alfredo González-Gil  
alfgonza@ucm.es  
Felisbina Luisa Queiroga  
fqueirog@utad.pt

Full list of author information is available at the end of the article



© The Author(s) 2024. **Open Access** This article is licensed under a Creative Commons Attribution-NonCommercial-NoDerivatives 4.0 International License, which permits any non-commercial use, sharing, distribution and reproduction in any medium or format, as long as you give appropriate credit to the original author(s) and the source, provide a link to the Creative Commons licence, and indicate if you modified the licensed material. You do not have permission under this licence to share adapted material derived from this article or parts of it. The images or other third party material in this article are included in the article's Creative Commons licence, unless indicated otherwise in a credit line to the material. If material is not included in the article's Creative Commons licence and your intended use is not permitted by statutory regulation or exceeds the permitted use, you will need to obtain permission directly from the copyright holder. To view a copy of this licence, visit <http://creativecommons.org/licenses/by-nc-nd/4.0/>.

## Background

Progress in stem cell-based research has led to a significant advance in regenerative medicine and cancer cell biology [1, 2]. Among adult stem cells harboured in different tissues, those committed to the neural lineage, neural stem cells (NSCs) and neural progenitor cells (NPCs), emerge as a very useful alternative tool to investigate in neurogenesis and neurodegenerative diseases [3]. Damaged neural cells renewal by NSCs/NPCs from brain neurogenic niches is poor [4], whereby extra-neural stem cells represent a valuable tool in autologous cell therapy. This has been reported for hair follicle [5], muscle [6], dental pulp [7], and ovarian cortical tissue [8, 9]. The isolation of adult stem cells followed by the specification and culture of generated NSCs/NPCs would accelerate research with a reduction in the use of laboratory animals, since adult stem cells can be obtained either by biopsy of tissues from alive animals or humans, or post-mortem.

Neurospheres (NS) are generated by spontaneous aggregation of NSCs/NPCs under certain culture conditions [7, 10] mediated by intercellular filopodial interaction or by membrane adhesion proteins [10]. Effective cell aggregation requires a minimum time and distance among nearby cells with subsequent changes in the actomyosin cytoskeleton that result in NS compaction [11]. As identifying hallmarks, NS are composed of NSCs and NPCs that express characteristic markers such as nestin, Sox2, and Pax6 and proliferate in response to neuronal induction and expansion factors [12]. NS-integrating cells can differentiate into neurons, and glial cells when they are cultured in appropriate differentiation media [8, 13]. The self-renewal ability and the capacity of NS cells to differentiate into neurons and glia can be assessed with the NS assay [14], an adequate method to identify molecules able to modify self-renewal and/or differentiation potential of NSCs/NPCs.

NS can be generated from sheep ovarian cortical cells (OCCs). In 21-days culture experiments, these NS (OCCs-NS) exhibit structural, ultrastructural, and molecular features of central nervous system (CNS)-NS, with self-renewal ability and capacity of NS-cells to differentiate into neurons and glia during the NS assay [8, 9]. Therefore, OCCs-NS may constitute a reliable alternative experimental model to investigate in neurogenesis and in CNS regenerative medicine [15].

The identification of proneurogenic and neuroprotective biomolecules, and their mechanisms of action is one of the key issues of current research on NSCs/NPCs [16, 17]. Different biomolecules and signalling pathways have been identified as involved in neurogenic processes [17] such as proliferation, survival, and neural differentiation [18]. However, the associated molecular mechanisms underlying most of their actions remain

poorly understood. The endocrine system is a regulator of neurogenesis [19, 20] as supported by the expression of different hormone receptors in CNS structures [18]. Particularly relevant actions are those of gonadotropin releasing hormone (GnRH) and steroid hormones, which stimulate certain processes of adult neurogenesis [18, 21, 22]. GnRH, known for its role in regulating the reproductive function through the hypothalamic-pituitary-gonadal axis, exerts neuromodulatory actions after binding on its brain receptors [23]. Gonadal steroid hormones are potent regulators of neurogenesis in adults. High levels of androgens enhance neurogenesis by increasing the survival of newly generated neurons [18, 24–26], either directly acting on new neurons by activation of the MAPK pathway, or indirectly, by increasing the expression of brain-derived neurotrophic factor (BDNF) [26, 27]. Oestrogens induce cell proliferation [27, 28] most probably after binding to oestrogen receptors  $\alpha$  and  $\beta$  [29] or indirectly through BDNF [30]. Oestrogen impacts on NSCs/NPCs proliferation in a dose-, oestrogen-type-, time-, species-specific, gender- and brain region-specific manner [18, 31]. Other hormones such as corticotropin-releasing hormone (CRH), thyroid hormones, glucocorticoids, leptin and ghrelin are also involved in specific processes of neurogenesis [18, 25, 32–35].

Follicle-stimulating hormone (FSH) secreted by the pituitary gland drives ovarian folliculogenesis by binding to the FSH receptor (FSHR). Even though its hypothetical role in neurogenesis has not yet been investigated, FSHR is localised in neurons of several CNS structures [36], like the hippocampus, site of one of the main neurogenic niches of the brain where NSCs/NPCs are involved in damaged neuron replacement [37]. Interestingly, FSH is involved in the pathophysiology of Alzheimer disease in mice since this hormone increases amyloid- $\beta$  and Tau deposition impairing cognition [36].

Ovarian surface epithelium (OSE) harbours two stem cell populations that express FSHR: very small embryonic-like stem cells (VSELs) and tissue-specific progenitors [38]. FSH stimulates asymmetric division of VSELs and symmetric division of progenitors, promoting their clonal expansion to thereafter differentiate into specific cell types [38, 39]. VSELs express transcripts of pluripotency such as *Oct4* and *Sox2*, upregulated by FSH after binding to FSHR [40, 41].

Since these cells, along with subpopulations of stem cells from ovarian cortical stroma, give rise to OCCs-NS (patent P2011601014/ES2605655A1) [8, 9], and preliminary experiments indicate that OCCs-NS exposed to FSH apparently reach larger diameters, it is hypothesised that FSH might exert proneurogenic actions on OCCs-NS, promoting differentiation of NSCs/NPCs in vitro. To date, this is the first study aimed to investigate the

hypothetical proneurogenic actions of FSH, using generation and culture of NS.

Therefore, the aim of this study was to elucidate whether FSH can stimulate self-renewal and exert growth-promoting and proneurogenic actions on NS generated in vitro from sheep OCCs, in long-term NS cultures and during the NS assay.

## Methods

### 21-days culture experiments

#### *Cell culture and generation of spheroids*

Ovaries obtained from ewe lambs (*Ovis aries*) aged 3–6 months, sacrificed at an abattoir, were aseptically dissected, transported to the laboratory at 2–8°C in 0.9% NaCl aqueous solution with 0.3067 g/l Penicillin (Sigma-Aldrich, Cat#P3032) and 0.6802 g/l Streptomycin (Sigma-Aldrich, Cat#S1277). Then, tissue was processed as previously described [8, 9]. From areas devoid of macroscopically visible antral follicles, 1 mm depth tissue strips from the ovarian cortex were dissected, fragmented into pieces of approximately 0.5×0.5 mm and collected in Dulbecco's modified Eagle's medium: F12 (DMEM: F12; Life Technologies, Cat#11039-021) with antibiotic-antimycotic 100x Solution (Gibco, Life Technologies, Cat#15240). For 30 min at 37 °C with gentle shaking, these fragments were disaggregated in Hank's Balanced Salt Solution with Calcium and Magnesium (Sigma-Aldrich, Cat#H9269) containing 0.6% collagenase type IA (125 CDU/mg; Sigma-Aldrich, Cat#C2674), 1% bovine serum albumin (BSA, Sigma-Aldrich, Cat#A9418), 100 IU/ml deoxyribonuclease (DNase, Sigma-Aldrich, Cat#D4513), and antibiotic-antimycotic. The resulting suspension was centrifuged, and supernatant was replaced with Hank's Balanced Salt Solution without Calcium and Magnesium (Sigma-Aldrich, Cat#H9394) with 1% BSA, 100 IU/ml of DNase and antibiotic-antimycotic. This suspension was centrifuged again, and the supernatant was replaced with DMEM: F12 with 0.1% BSA, 3 mM L-glutamine (Sigma-Aldrich, Cat# G7513), 10 µl/ml insulin, transferrin, and selenium (ITS, Sigma-Aldrich, Cat#I3146), 2 µl/ml Synthecol (Sigma-Aldrich, Cat#S5442) and antibiotic-antimycotic. This suspension was filtered successively through 100-, 70- and 40-µm cell strainers (Becton Dickinson, BD Falcon, Cat#352,360, Cat#352,350, and Cat#352,340, respectively).

Trypan blue (Sigma-Aldrich, Cat#T8154) staining was performed on an aliquot of the cell suspension to determine the concentration of alive cells after counting them in a haemocytometer. Then, 500,000 alive cells were seeded per well. Two defined media were used: (a) Control group (C-group) medium composed by DMEM: F12, 0.1% BSA, 3 mM L-glutamine, 10 µl/ml ITS, 2 µl/ml Synthecol, and antibiotic-antimycotic; (b) FSH group (FSH-group) medium with the same composition as C-group

medium supplemented with 50 ng/ml ovine FSH (NIDDK, Cat#NIDDK-oFSH-18AFP5862D). Cells were cultured for 21 days at 37 °C, 5% CO<sub>2</sub>, and 99% humidity in a Forma Steri-Cycle incubator (Thermo Scientific Forma). Culture medium was replaced every 48 h with fresh medium with the same composition.

#### *Experimental designs*

Image analysis and morphometric evaluation were performed every 48 h. Gene expression and immunohistochemical analyses were carried out on RNA extracts obtained on days 0, 10, 15, 21 and on NS-tissue sections, of days 10, 15 and 21 of culture, respectively.

#### *Image analysis of NS development in vitro*

Cultures were observed and photographed under an inverted microscope (Nikon Eclipse TiS) provided with a digital camera (Nikon DS-Fi1) and image analysis software (NIS-D-Elements, Nikon). Diameters of, at least, 200 NS were measured at each time-point, as previously described [8].

#### *Immunohistochemical analyses*

Immunohistochemical analyses were performed following a previously established procedure (Patent P201300524/PCT/ES2014/000089) [8]. NS sections were covered with diluted primary antibodies previously validated: polyclonal rabbit anti-Pax6 antibody (1:400; Sigma-Aldrich, Cat#030765) and mouse monoclonal anti-nervous growth factor receptor (1:1500; p75NTR; Sigma-Aldrich, Cat#N3908), were incubated in humidified chamber overnight at 4 °C; rabbit polyclonal anti-*nestin* (1:200; Sigma-Aldrich, Cat#N5413) and mouse monoclonal anti-vimentin (1:500; clone V9; Dako), were incubated 1 h at room temperature.

At least 10 sections per time-point were used for immunolocalization of each marker. Image analyses were performed under an Olympus DP50 microscope, provided with a digital camera (Olympus), and software Viewfinder Lite and Studio Lite (Better Light Inc). Positive and negative cells were counted in each tissue section and their percentages were calculated for each marker at each time-point.

#### *Gene expression analyses*

Cell lysates were obtained from cell suspension before culture (day 0) and from NS contained in 3 culture wells per time-point and were stored frozen at -80°C until RNA extraction, as previously described [8].

Ovine transcripts quantified by quantitative Reverse Transcription Polymerase Chain Reaction (qRT-PCR) were: octamer binding transcription factor 4 (*Oct4*), homeobox transcription factor (*Nanog*), sex determining region Y-box 2 (*Sox2*), *nestin*, *vimentin*, paired box 6

(*Pax6*), neurotrophin receptor p75 (*p75NTR*), neural precursor specific transcript doublecortin (*DCX*), astrocyte/radial glia characteristic transcript, glial fibrillary acidic protein (*GFAP*), oligodendrocyte specific transcript *Olig2*, alpha-fetoprotein (*AFP*; endoderm specification transcript), *brachyury* (mesoderm specification transcript), FSH receptor (*FSHR*), and *18 S ribosomal RNA* as endogenous control. Analyses were carried out at Antonia Martín Gallardo Genomics and Proteomics Service (Scientific Park of Madrid) as previously described [8].

The primers used for amplification (Supplementary Table 1) were synthesised on the basis of mRNA sequences available at the National Centre for Biotechnology Information.

For time-dependent relative quantification (RQ) of each transcript, the levels of transcription of the gene on day 0 were used as reference. For RQ of all transcripts within each time-point the gene with lowest expression, *brachyury* in C-group, was used as reference.

#### NS assay

NS assay was based on previously established procedures [8, 42]. After isolation as described above, 500,000 and 20,000 alive cells were plated per well in fibronectin-coated 24- and 96-well plates, respectively. The NS assay comprised two subsequent periods of 7 days of culture for cell expansion (CEP-1, CEP-2) with one of three defined media (groups): (a) M1 (control medium for cell expansion and neural induction) composed by DMEM: F12, 0.1% BSA, 1% N2 (Life Technologies, Cat#17502048), 3 mM L-glutamine, 20 ng/mL epidermal growth factor (EGF, Sigma-Aldrich, Cat#E9644), 20 ng/mL fibroblast growth factor 2 (FGF2, Sigma-Aldrich, Cat#F0291) and antibiotic-antimycotic; (b) M2, with the same composition as C-group medium (Sect. 2.1.1); (c) M3, with the same composition as FSH-group (Sect. 2.1.1). Cells were cultured at 37 °C, 5% CO<sub>2</sub> and 99% humidity.

On day 7 of CEP-1, part of the NS1 were disaggregated with Accutase (Stem Pro Accutase, Life Technologies, Cat#A1110501), and subcultured to initiate CEP-2 and generate NS2.

For assessment of NS generation, image analysis was performed every 48 h. Proliferative activity of cells was assessed on day 5 in both CEP, on cells seeded in 96-well plates ( $n=8$  culture wells/group) using a bromodeoxyuridine (BrdU) uptake enzyme immunoassay (Abcam, Cat#ab126556), as previously described [8]. Self-renewal of NS1 was determined by the ability of cells to proliferate and to generate NS2, with similar gene expression profiles than NS1. For this purpose, total RNA was extracted from NS1 and NS2 lysates on day 7. *Sox2*, *Oct4*, *Nanog*, *nestin*, *Pax6*, *p75NTR*, *DCX*, *GFAP*, *Olig2*, and *18 S ribosomal RNA* (endogenous control) were quantified by qRT-PCR, as described above (Sect. 2.1.5.). The primers

used for amplification are shown in Supplementary Table 1. For the RQ of each transcript its level of expression in M1 was considered as reference. For the RQ of all transcripts within each time-point, the level of expression of *Nanog* for each group was used as reference.

On day 7 of CEP-2, NS2 were treated with Accutase to obtain isolated cells. After Trypan Blue viability test, 80,000 alive cells/cm<sup>2</sup> were seeded on 12-mm round borosilicate coverslip (Menzel, Thermo Fisher Scientific, Cat#CB00120RAC20MNTO) pre-coated with polyornithine-fibronectin that has been inserted into each well of 24-well culture plates. Cells were cultured in DMEM: F12 with 2% foetal bovine serum (Life Technologies, Cat#A3160401), 1% N2 supplement, 3 mM L-glutamine, and antibiotic-antimycotic. From day 15 of culture onwards, EGF receptor antagonist (CP-380736, 100 μM, Sigma-Aldrich, Cat#PZ0129) and FGF2 receptor antagonist (SU5402, 100 μM, Sigma-Aldrich, Cat#SML0443) were added to the medium. Cells were cultured at 37 °C, 5% CO<sub>2</sub> and 99% humidity for 25 days. Medium (2/3 of volume) was replaced every 48 h by fresh medium with the same composition. Image analyses were performed every 48 h, and the presence of glial cells and mature neurons was assessed on day 25 of culture by immunofluorescent staining of GFAP, and NeuN, respectively following a previously set-up procedure [8]. Cells were incubated with fluorochrome-conjugated antibodies diluted in 5% BSA-PBS. Anti-NeuN (1:300; Abcam, Cat#ab177487) was labelled with DyLight 488 (Abcam, Cat#ab201799), and anti-GFAP (1:200; Sigma-Aldrich, Cat#G4546) with DyLight 594 (Abcam, Cat#ab201801). An *Olig2* antibody with reactivity in sheep was not available. After overnight incubation with antibodies, washing, counterstaining with DAPI and mounting, glass slides were stored in the dark at 2–8 °C until image analysis in a confocal laser microscope (Leica TCS SP8; Leica Microsystems 2.8; Centre for Fluorescence Cytometry and Microscopy, Complutense University of Madrid).

#### Statistical analyses

Changes in NS diameters were analysed by two-way ANOVA ( $p<0.01$  was significant). Variations in percentages of immunolocalization of NSC/NPC antigens were analysed by Kruskal Wallis non-parametric tests after assessment of data normal distribution with the Shapiro–Wilk test ( $p<0.05$  was significant). RQ of each transcript with respect to its expression at day 0 in each group (21-days cultures) was analysed by one-way ANOVA ( $p<0.01$  was significant). RQ of all transcripts at each time-point were compared by non-parametric multiple comparisons test with differences significant at  $p<0.05$ . Non-parametric Kruskal–Wallis test was performed to assess the effect of group (C vs. FSH) on RQ of each transcript at each time-point (*brachyury* in C-group was

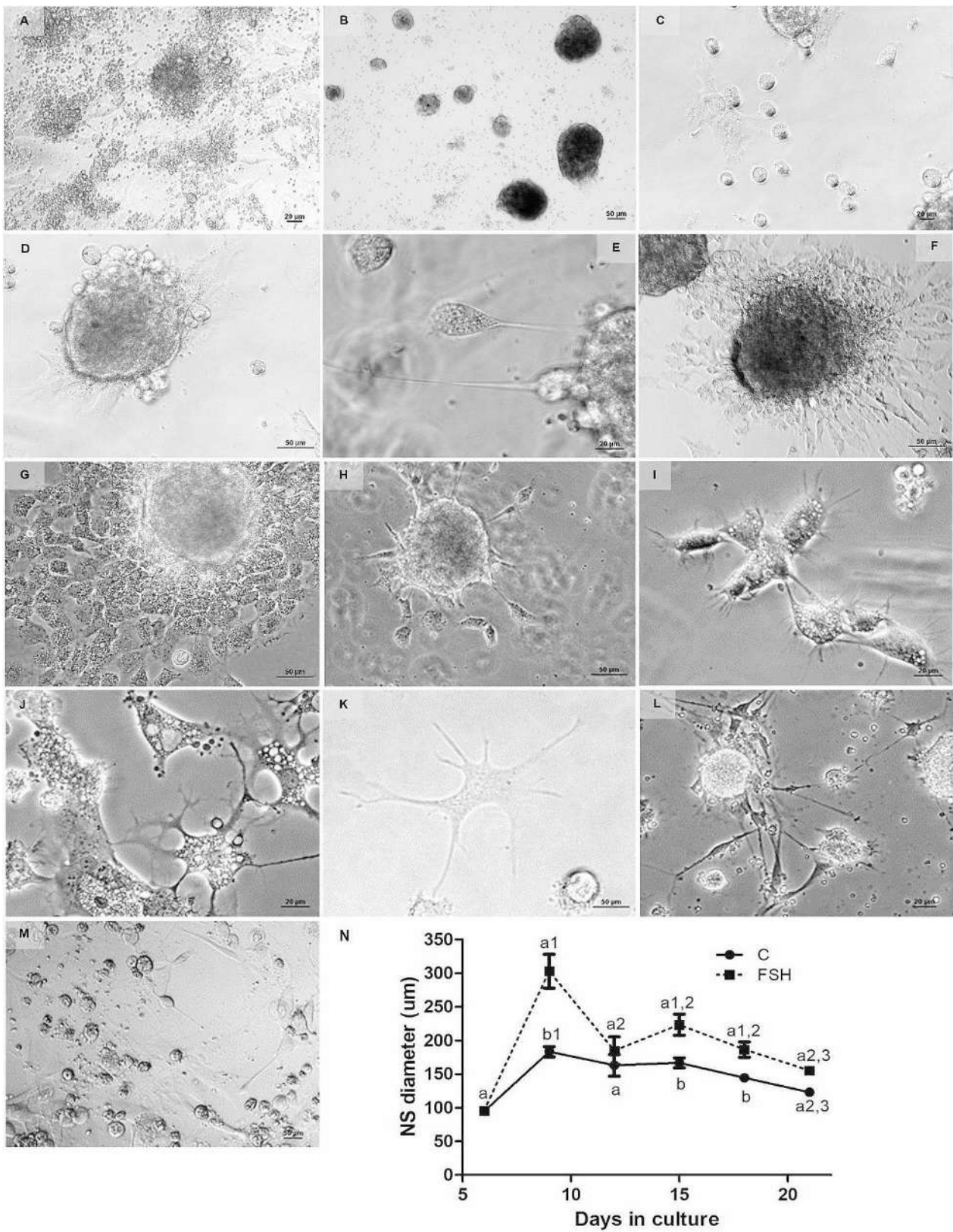


**Fig. 1** (See legend on next page.)

(See figure on previous page.)

**Fig. 1** Photomicrographs corresponding to 21-days culture experiments, showing cell aggregation on 72 h after cell seeding (**A**, C-group; phase contrast, 20X/0.40 magnification), followed by formation of compact spheroids on day 6 of culture (**B**, C-group; phase contrast, 10X/0.22 magnification). On days 10 and 20 of culture, round polarized cells with large nucleus/cytoplasm ratio, exhibited consistent patterns of migration from one NS to another one (**C**, FSH-group; phase contrast 20X/0.40 magnification), and apparently joined to the outer cell layer of a pre-existing NS (**D**, FSH-group; phase contrast 20X/0.40 magnification). From 13 days in culture, cells from the outer NS layer showed signs of morphological differentiation (**E**, C-group; phase contrast 40X/0.55 magnification; **F**, FSH-group; phase contrast 20X/0.40 magnification), to thereafter migrate from the NS to the surrounding growth surface (**G**, FSH-group; phase contrast 20X/0.40 magnification). Cells from the NS-outer sheet cover exhibited projections like neurites at their apical membrane (**H**, phase contrast 20X/0.40 magnification). Cells arising from NSs differentiated on growth surface (**I**; phase contrast 40X/0.55 magnification), into cells morphologically similar to mature astrocytes (**J**, **K**; phase contrast 40X/0.55 magnification), and neurons (**L**; phase contrast; **M**; Hoffman, both 20X/0.40 magnification). **N**: Line-graph depicting time-course variation in NS diameters ( $\mu\text{m}$ ; mean  $\pm$  SE) in C-group and FSH-group. Different letters (**a**, **b**) indicate significant differences ( $p < 0.05$ ) between both groups at each time-point. Different numbers (1, 2, 3) indicate time-dependent differences ( $p < 0.05$ ) within each group compared with diameters on days 6, 9 and 15, respectively. NS, neurosphere

used as reference gene;  $p < 0.05$  was significant). Studied genes were grouped into five clusters of lineages and/or developmental status (endoderm, mesoderm, NSC/NPC, neural differentiating cells, and pluripotent cells), cluster-dependent differences being determined by non-parametric multiple comparisons tests ( $p < 0.05$  was significant). The effect of group (C vs. FSH) was determined by non-parametric Kruskal-Wallis test with significance at  $p < 0.05$ . For NS assay data, both the effect of group and group-dependent changes on RQ of each transcript in NS1 and NS2, were determined by one-way ANOVA ( $p < 0.001$  and  $p < 0.05$  were significant, respectively). Group-dependent variations in cell proliferation assays were compared by two-way ANOVA being differences significant with  $p < 0.05$ . In all cases, Bonferroni post-hoc tests were done after ANOVA, which was performed using Graph-Pad Prism 4 software. Non-parametric tests for RQ analyses were carried out with S.A.S.

## Results

### FSH promotes development of OCCs-NS generated in vitro

Spontaneous cell aggregation occurred from 24 h after the onset of culture, being most evident at 72 h (Fig. 1A). Cell aggregates became spheroids on days 5–7 of culture (Fig. 1B). Approximately, 65 to 75 spheroids were generated from every 500,000 cells seeded. Microscopy observations evidenced abundant big round cells with large ratio nucleus/cytoplasm migrating from one NS to another (Fig. 1C, D), around days 10 and 20 of culture. These cells exhibited an organised path of migration, and signs of polarisation, like cytoskeleton structures placed at the front pole of the cell, and a backward positioned nucleus (Fig. 1C, D), apparently becoming attached to the periphery of a pre-existing NS (Fig. 1D). From day 13 of culture, cells at the outer layer of NS showed elongating projections directed towards the NS periphery (Fig. 1E, F), and appeared to migrate to the surrounding growth surface displaying numerous short and thin projections on their apical membrane that resembled neurites, and abundant cytoplasmic lipid-like droplets (Fig. 1G–I). Finally, cells with astrocytic (Fig. 1J, K) and neuronal morphology (Fig. 1L, M) covered the growth

surface from 15 days of culture. In the FSH-group there were more migratory cells, NS were larger, and they established more frequent contacts with neighbouring NS. NS-diameters were greater in FSH-group than in C-group from day 9 of culture ( $302.90 \pm 25.20 \mu\text{m}$  vs.  $183.20 \pm 7.63$ , respectively;  $p < 0.05$ ) onwards (Fig. 1N).

### FSH regulates transcripts of pluripotency and neuroepithelial cell lineage in OCC-NS

*Oct4*, *Sox2* and *Nanog* were expressed during the whole culture, with up-regulation of *Sox2* ( $p < 0.05$ ) and down-regulation of *Oct4* ( $p < 0.05$ ) and *Nanog* ( $p < 0.05$ ) on day 10, regardless of FSH addition. *Sox2* transcription (Fig. 2A) was increased ( $p < 0.05$ ) on day 21 in FSH-group compared with C-group. *Oct4* (Fig. 2B) and *Nanog* (Fig. 2C) expression decreased from day 0 to 15 ( $p < 0.05$ ) in both groups and increased on day 21 ( $p < 0.05$ ), being *Oct4* mRNA levels higher in FSH-group ( $p < 0.05$ ).

Expressions of *AFP* (Fig. 2D), and *brachyury* (Fig. 2E) were close to the detection limit of the technique and were upregulated on day 21 in both groups ( $p < 0.01$ ) with increased expression of both transcripts in FSH-group ( $p < 0.05$ ).

Time-course expression of NSC/NPC transcripts (Fig. 2F–I) showed that *nestin* (Fig. 2F) was upregulated in both groups being higher in FSH-group than in C-group on days 15 and 21 ( $p < 0.01$ ). *Pax6* transcription was upregulated from day 10 in both groups, being higher in FSH-group than in C-group on days 15 and 21 ( $p < 0.01$ ) (Fig. 2G). Expression of *p75NTR* (Fig. 2H) was upregulated on day 10 in both groups but then showed a downward trend, with lower expression in FSH-group on day 15 ( $p < 0.05$ ). *Vimentin* had an upward trend as culture progressed up to 15 days in FSH-group and 21 days in C-group when its transcription was larger than in FSH-group (Fig. 2I).

*DCX* (Fig. 2J), *GFAP* (Fig. 2K), and *Olig2* (Fig. 2L) were upregulated on day 10 in culture, with levels of expression higher than those of day 0, 15, and 21 ( $p < 0.01$ ) in both groups.

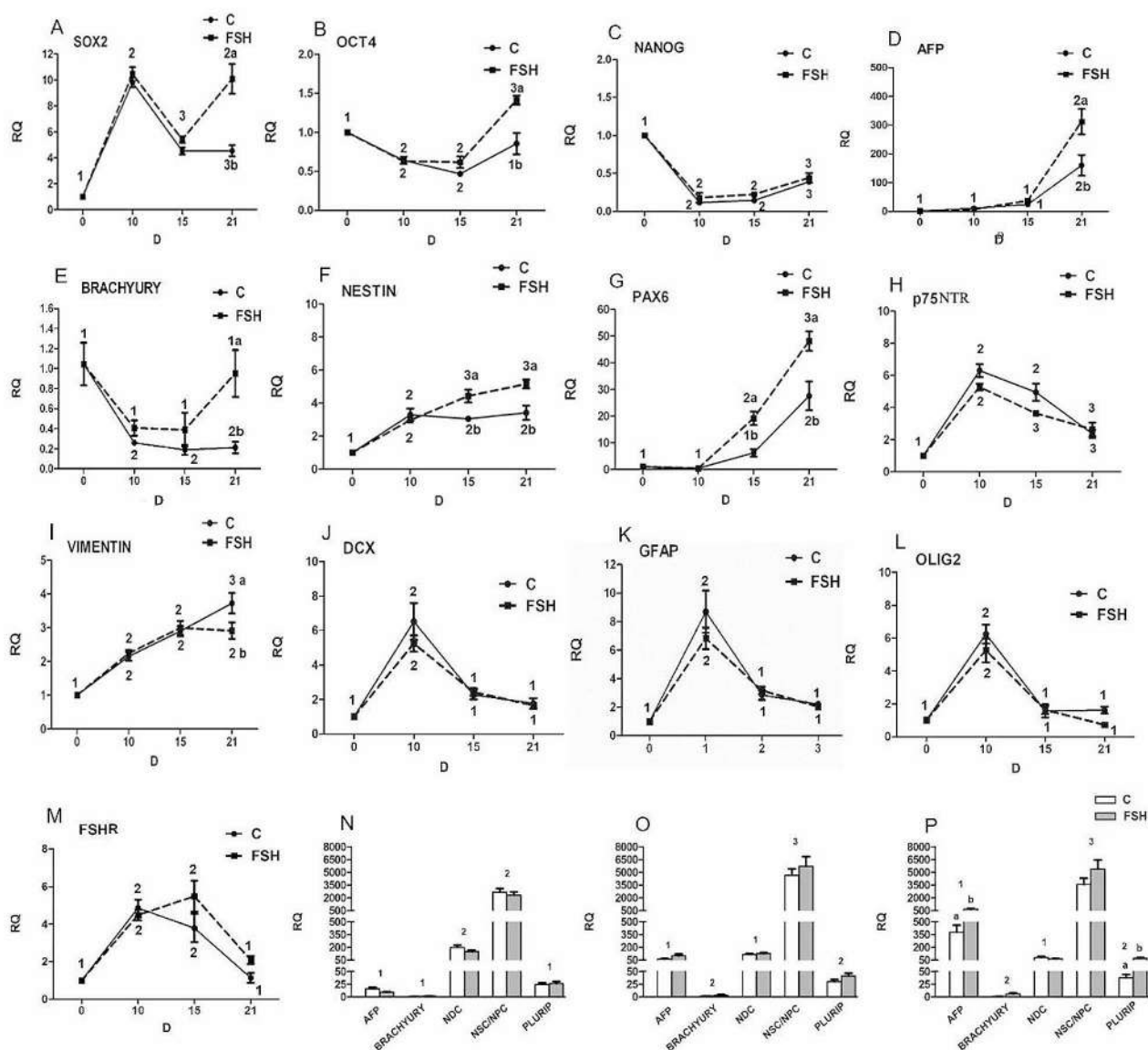


**Fig. 2** Line-graphs depicting RQ of analysed transcripts by quantitative RT-PCR, during 21-days culture experiments. Each value represents the mean RQ of each gene at each time-point of analysis (days in culture, **D**) with respect to its levels on day 0 in C-group and FSH-group. Different numbers (1, 2, 3) or letters (**a**, **b**) indicate time- and group-dependent significant differences ( $p < 0.01$ ) in expression of each transcript, respectively. Histograms showing RQ of transcripts grouped in clusters of genes characteristic of endoderm (*AFP*), mesoderm (*brachyury*), neural differentiating cells (NDC: *DCX*, *GFAP*, *Olig2*), NSC/NPC (*nestin*, *p75NTR*, *Pax6*), and pluripotent cells (PLURIP: *Sox2*, *OCT4*, *Nanog*) within each time-point of analysis, day 10 (**N**), day 15 (**O**), and day 21 (**P**) in C- and FSH-group. *Brachyury* was used as reference for RQ of all other transcripts in clusters. Different numbers over the bars indicate significant differences ( $p < 0.05$ ) in gene expression with respect to that of reference for comparison (*brachyury* in C-group). Different letters denote differences ( $p < 0.05$ ) between C- and FSH-group. RQ, relative quantification; RT-PCR, reverse transcription polymerase chain reaction

*FSHR* (Fig. 2M) was similarly expressed in C- and FSH-groups ( $p > 0.05$ ), with increased levels on day 10 and 15 of culture over those on day 0 ( $p < 0.01$ ), and 21 ( $p < 0.01$ ).

RQ of all transcripts within each time-point of analysis is presented in Supplementary Fig. 1. Maximum transcription was that of *vimentin*, followed by *nestin*, *Pax6*, *p75NTR*, *DCX*, *GFAP* and *Olig2*.

NSC/NPC transcripts showed the highest expression ( $p < 0.05$ ) throughout the culture, followed by NDC

genes, then *AFP* and pluripotency transcripts, and finally *brachyury* (Fig. 2N-P). FSH increased ( $p < 0.05$ ) the expression of pluripotency and *AFP* genes compared with C-group on day 21 (Fig. 2P).

#### FSH influences the expression of NSC/NPC antigens in OCC-NS

Nestin, *Pax6*, *p75NTR*, and *vimentin* were immunolocalized in NS from C- and FSH-groups throughout the

whole culture (Fig. 3). Nestin and Pax6 (Fig. 3A and B, respectively) showed nuclear localization; p75NTR displayed nuclear staining and, to a lesser extent, cytoplasmic (Fig. 3C); and vimentin showed cytoplasmic staining (Fig. 3D).

Percentages of NS-cells immunolocalizing NSC/NPC antigens are presented in Fig. 3E-H. On day 10, FSH reduced the percentage of nestin-positive NS-cells when compared to control ( $p < 0.05$ ). However, on day 21, FSH raised the percentages of nestin-positive NS-cells with respect to C-group ( $p < 0.05$ ). FSH decreased ( $p < 0.05$ ) the percentages of Pax6-positive NS-cells compared with C-group on days 10 and 15 ( $77.61 \pm 3.5$  in FSH-group vs.  $88.29 \pm 1.5$  in C-group, on day 10) and increased it on day 21 ( $94.05 \pm 0.3$  vs.  $85.65 \pm 1.6$ ;  $p < 0.05$ ) compared with C-group and with respect to previous percentages in FSH-group. Finally, cell counts of p75NTR-positive and vimentin-positive NS-cells were similar at all time-points in both groups, with the only exception of a larger percentage ( $p < 0.05$ ) of p75NTR-positive NS-cells in C-group on day 10 with respect to FSH-group ( $85.23 \pm 3.4$  vs.  $73.17 \pm 4.6$ ).

### Neurosphere assay

OCCs began to aggregate 24 h after the onset of culture in both CEP to generate clusters at 72 h and compact NS 5–6 days after seeding in all groups (Fig. 4C-E). NS diameters increased after seeding in both CEP in all groups (Fig. 4A, B). During CEP-1, NS-diameters were larger in M1 than M3 on days 3 and 7 ( $p < 0.05$ ; Fig. 4A). On CEP-2, NS-diameters were larger in M2 and M3 than M1 on day 3 ( $p < 0.05$ ) and reached maximum and similar diameters on day 7 (Fig. 4B).

Cells from all groups exhibited proliferative activity during both CEP (Fig. 4F, G). In CEP-1, M1 and M3 cells showed values larger than those of M2 cells ( $p < 0.05$ ). In CEP-2, M3 cells showed increased BrdU incorporation with respect to cells from M1 and M2 ( $p < 0.05$ ), being M1 values lower than M2 ( $p < 0.05$ ) (Fig. 4G). Image analysis demonstrated that cells exposed to EGF and FGF2 in CEP-2 became confluent on day 3 of culture.

RQ of transcripts of pluripotency, endoderm, mesoderm, NSC/NPC, and neural differentiation in NS1 and NS2 are presented in Fig. 5. *Nestin* was the most expressed transcript in all groups ( $p < 0.01$ ) during both CEP while transcription of *AFP* and *brachyury* were close to the detection limit of the technique.

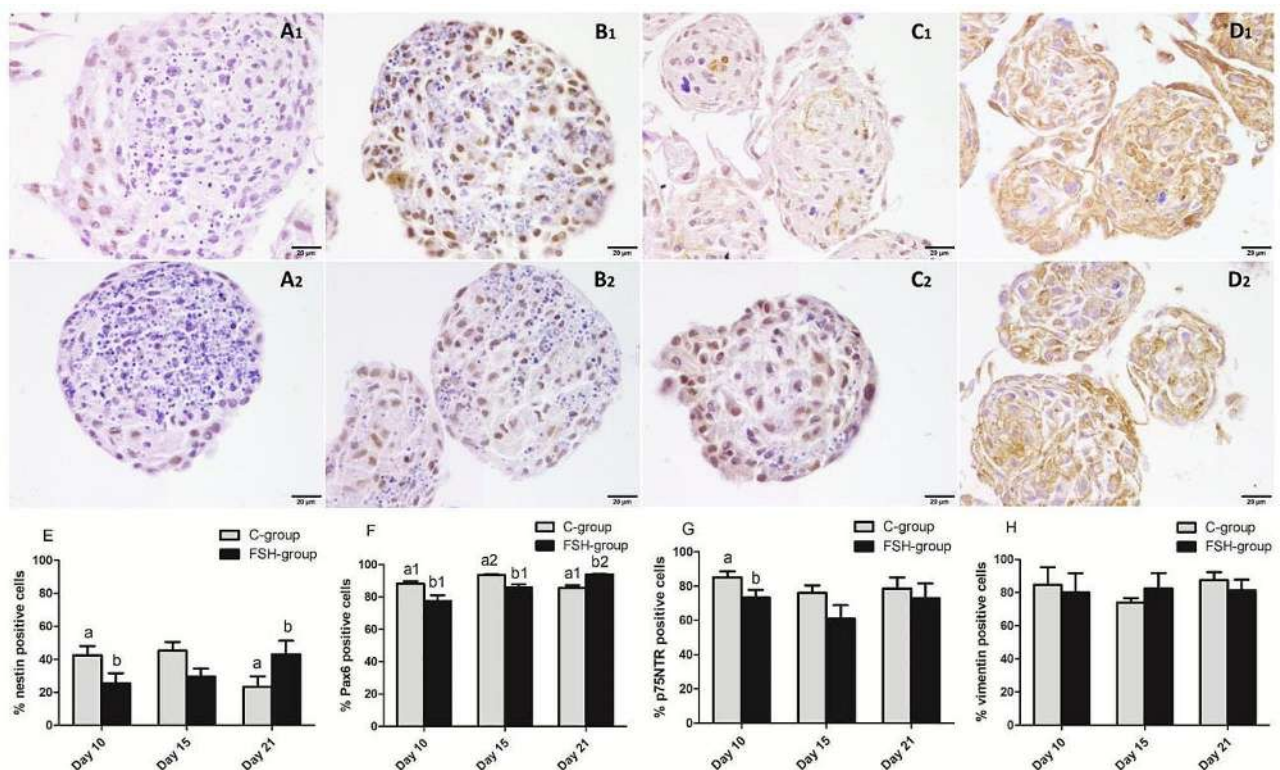


**Fig. 3** Photomicrographs of NS cultured in serum-free medium control (first row, subindex 1) or supplemented with FSH (second row, subindex 2) on day 10 of culture showing immunolocalization of nestin (A), Pax6 (B), p75NTR (C), and vimentin on day 21 (D). Histograms depicting percentages of NS-cells that immunolocalized the NSC/NPC antigens nestin (E), vimentin (F), Pax6 (G), and p75NTR (H) during culture in C- and FSH-group on days 10, 15, and 21 of culture. Different number or letter superscripts indicate time-dependent significant differences ( $p < 0.05$ ) for each antigen within each group or between groups at each time-point, respectively. NS, neurosphere; NPC, neural progenitor cell; NSC, neural stem cell

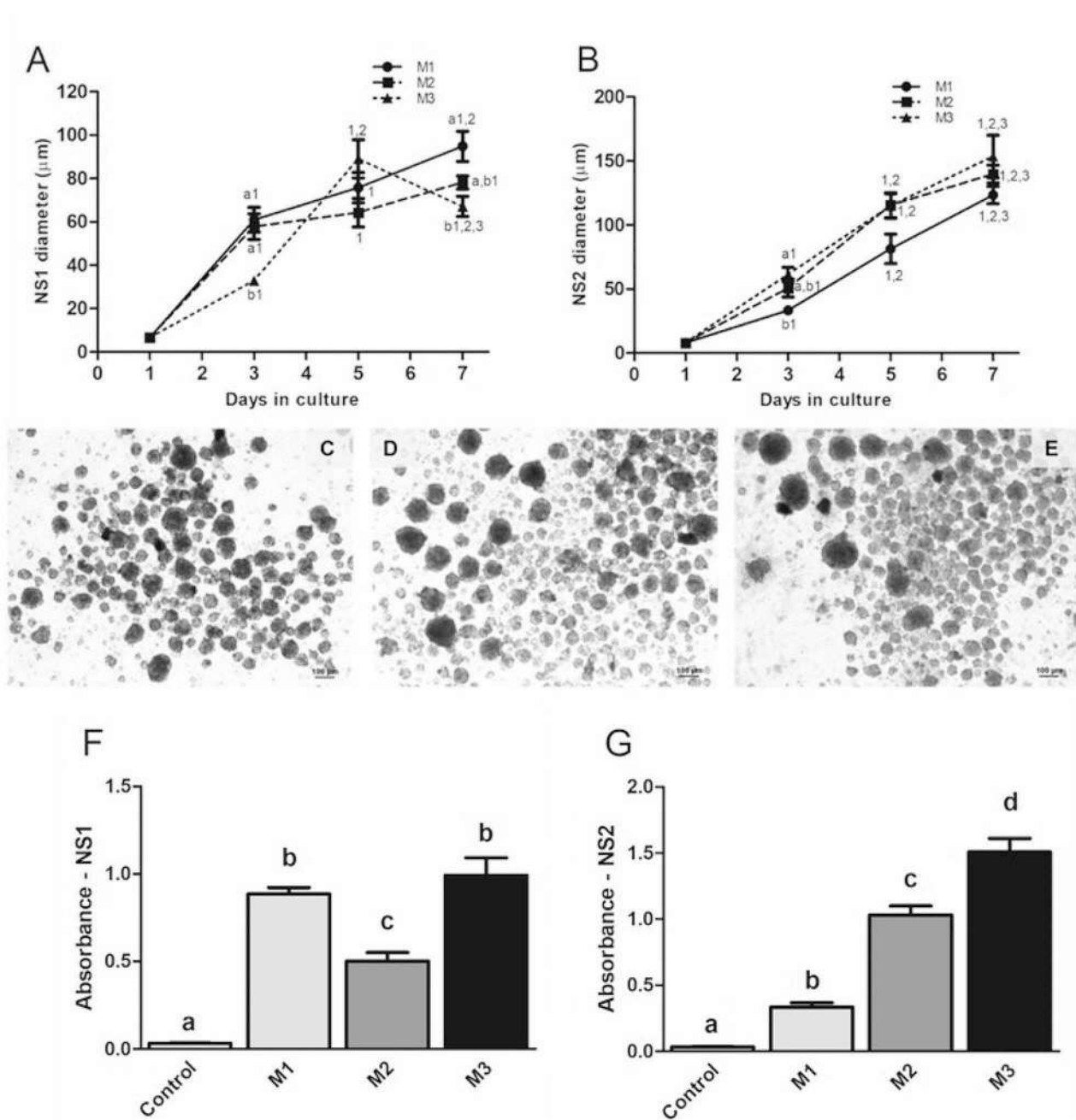


**Fig. 4** Time-dependent variations of NS1 (A) and NS2 (B) diameters (µm; mean ± SE) in M1, M2 and M3, during the first and second cell expansion periods (CEP-1 and CEP-2, respectively). Different letters (a, b) indicate group-dependent significant differences ( $p < 0.05$ ) at each time point. Different numbers (1, 2, 3) indicate time-dependent differences ( $p < 0.05$ ) within each group: 1 compared with diameters on day 1; 2 compared with diameters on day 3; and 3 compared with diameters on day 5. Photomicrographs (10X/0.22 magnification, phase contrast) showing compact NS formed in vitro approximately 6 days after seeding in M1 (C), M2 (D) and M3 (E). Cell proliferation assays showing BrdU incorporation on day 5 of culture during CEP-1 (NS1; F) and CEP-2 (NS2; G). Each bar represents the absorbance (mean ± SE) measured in M1, M2, and M3. Cells exposed to culture medium without BrdU were used as negative control. Different letters (a, b, c) indicate significant differences ( $p < 0.05$ ) among values. NS1 and NS2, primary and secondary neurospheres, respectively

NS1 from M2 showed larger expression of *p75NTR*, *DCX*, *Olig2* and *GFAP* ( $p < 0.01$ ) than in M1 (Supplementary Fig. 2F-I, respectively), and larger expression of nestin, *DCX* and *GFAP* ( $p < 0.01$ ) than in M3 (Supplementary

Fig. 2D, G, H, respectively). Regarding NS2, FSH down-regulated ( $p < 0.05$ ) the expression of *Sox2* and *Oct4* and upregulated *Nanog* ( $p < 0.05$ ) when compared with M1 and M2 (Supplementary Fig. 3A-C). The expression of

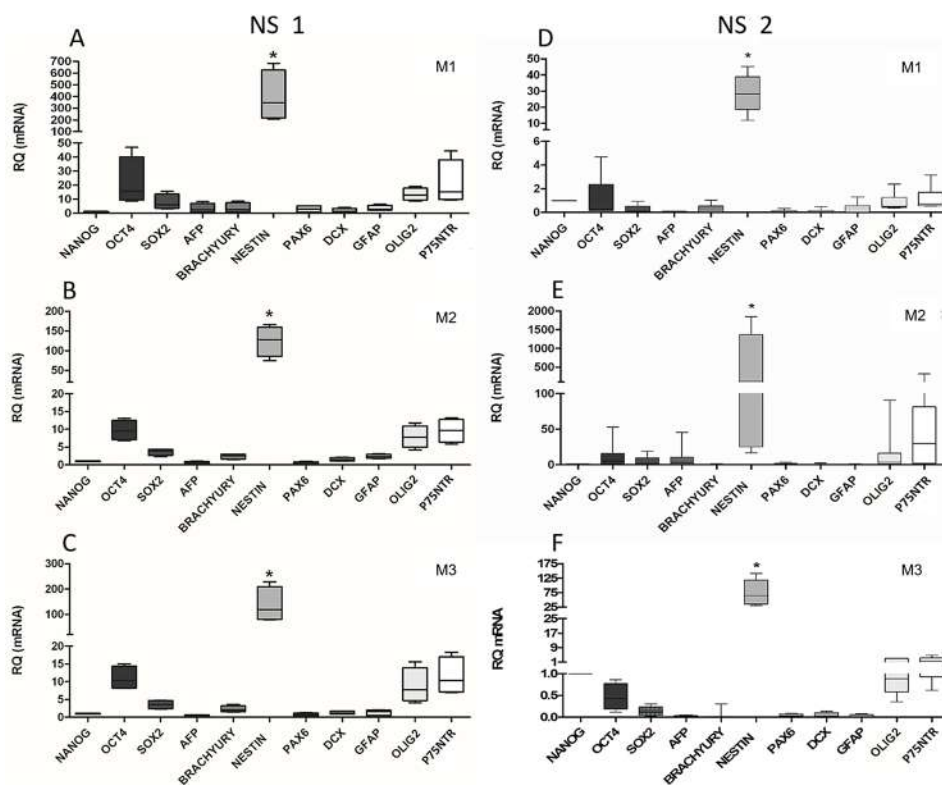


**Fig. 5** Relative quantification (RQ) of transcripts characteristic of pluripotency (*Nanog*, *Oct4*, *Sox2*); endoderm (*Afp*), mesoderm (*brachyury*), NSC/NPC (*nestin*, *Pax6*, *P75NTR*) and neural differentiation (*Dcx*, *Gfap*, *Olig2*) in NS1 and NS2 from M1 (A, D), M2 (B, E) and M3 (C, F), by quantitative RT-PCR. Results are presented in box plot format, with median, minimum, maximum value, and standard error for each transcript. *Nanog* expression was used as reference for normalization. Asterisk (\*) indicates significant differences ( $p < 0.05$ ) between *nestin* expression and all the transcripts analysed. RT-PCR, reverse transcription polymerase chain reaction; NPC, neural progenitor cell; NSC, neural stem cell; NS1 and NS2, primary and secondary neurospheres, respectively

*DCX* in M1 and M3 was greater than that found in M2 ( $p < 0.05$ ) while that of *GFAP* was larger in M1 than M2 and M3 ( $p < 0.05$ ) (Supplementary Fig. 3G, H, respectively). In NS2, *nestin* expression increased ( $p < 0.01$ ) over levels quantified in NS1, whereas the expression of transcripts characteristic of differentiation showed a reduction ( $p < 0.01$ ) in NS2 compared with those in NS1 (Supplementary Figs. 3 and 4).

Microscopy observations evidenced that, up to 48–72 h after the onset of culture in both CEP, the growth surface was covered by spindle-shaped cells, closely surrounded by very small round cells that apparently established a paracrine interaction (Fig. 6A). From 72 h onwards, large round cells with a high ratio nucleus to cytoplasm aggregated (Fig. 6B) to generate spheroids that became compacted on day 6 of culture (Fig. 6C). Mitotic events were frequently observed during both CEP (Fig. 6D, E).

During culture for differentiation, no significant changes in cell morphology were evidenced before addition of EGF and FGF2-antagonists to defined medium (Fig. 6F). From twelve hours after exposure of cells to these antagonists, there were notorious changes in the shape of cells. Round cells arising from the NS or lying on

the surrounding growth surface showed neural-like morphological differentiation. Short projections like filopodia began to appear around the cells (Fig. 6G, H). Later, many of the cells exhibited a single elongated projection at one pole and small neurite-like projections at the opposite one (Fig. 6I). It was frequent to find spindle-shaped neuroblast-like cells (Fig. 6J), either alone or grouped in chains. Residual NS formation remained during the first 10 days of culture for differentiation. Interestingly, long projections were observed that connected close or distant NS, giving rise to a dense net of cell-bridges over the growth surface. This finding was particularly relevant in M3 at the end of culture (Fig. 6K–M). These projections were used by round cells with a high nucleus/cytoplasm ratio that came out from a NS, or aggregated to it, to get attached and apparently migrate (Fig. 6L, M). Cells with neuronal and astrocytic morphology covered the growth surface, from approximately the middle of this period of culture, particularly in M3 (Fig. 6N, O).

On day 25 of culture, most cells showed cytoplasmic and/or nuclear immunolocalization of NeuN, a characteristic antigen of differentiated neurons, and many cells displayed cytoplasmic immunolocalization of astrocyte

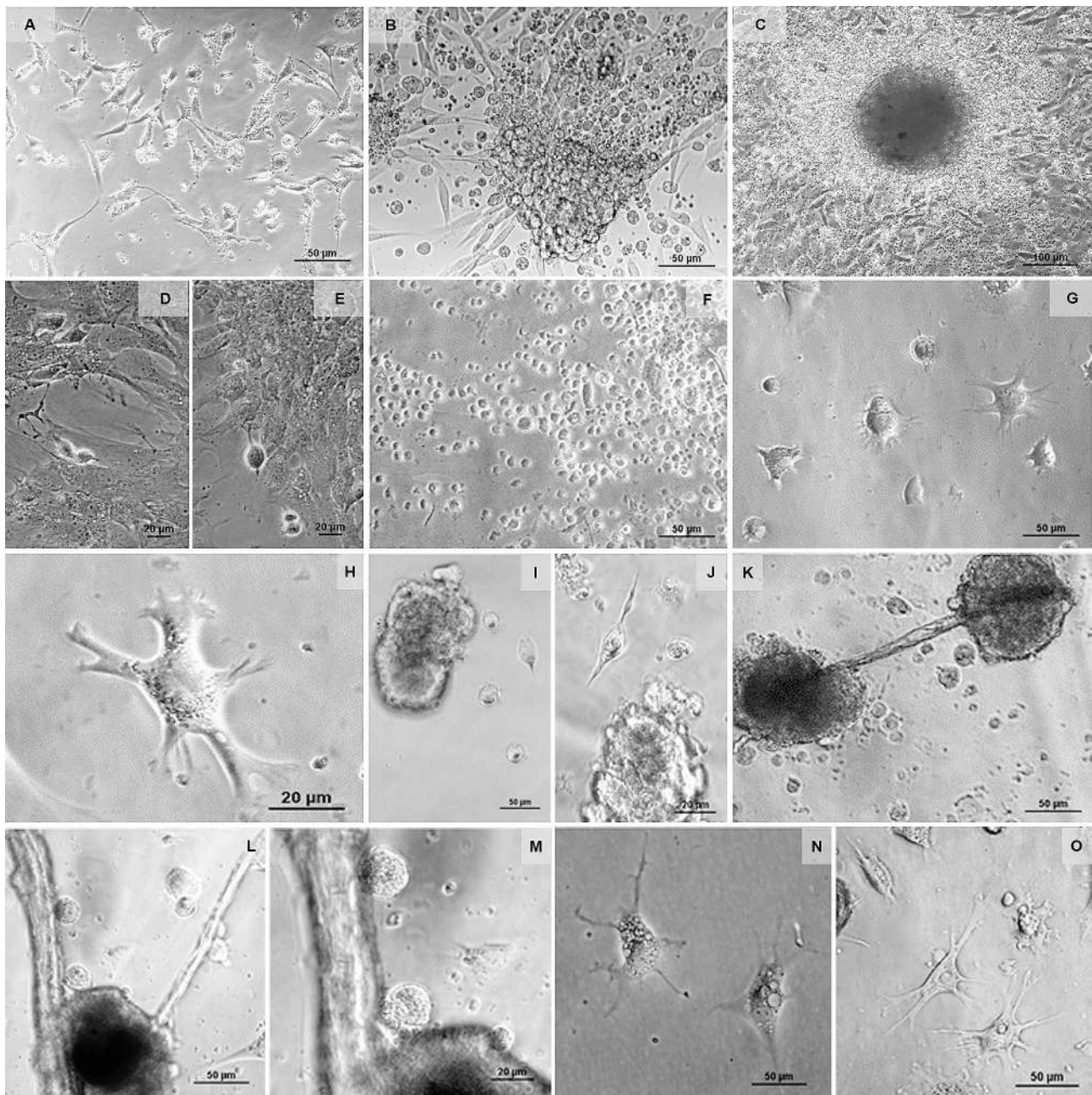


**Fig. 6** Photomicrographs taken during the expansion periods showing very small round cells closely attached to stromal cells 72 h after culture onset (A, phase contrast 10X/0.22 magnification). Big round cells aggregate (B, Hoffman, 20X/0.40 magnification) to generate spheroids that become compacted on day 6 of culture (C, phase contrast 10X/0.22 magnification). During both expansion periods mitoses were frequently observed (D, E, phase contrast 20X/0.40 magnification). Photomicrographs taken during culture for differentiation, showing absence of morphological changes in cells before addition of EGF and FGF2 antagonists to the medium (F, phase contrast, 10X/0.22 magnification), and initiation of morphological differentiation of cells from 12 h onwards (F-O), with most cells exhibiting cell projections to acquire a neural-like morphology (G, phase contrast 20X/0.40 magnification; H, phase contrast 40X/0.55 magnification). Neuroblast-like cells (I, J, phase contrast 20X/0.40 magnification) were frequently found. Extensive projections arising from NS established contact with neighbouring NSs (K-M), where cells with a high nucleus/cytoplasm ratio (M, N) attached to it and migrated (L, phase contrast 20X/0.40 magnification; M, phase contrast 40X/0.55 magnification). Differentiated cells with neuronal and astrocytic morphology covered the growth surface from mid to the end of differentiation culture period (N, phase contrast 20X/0.40 magnification; O, Hoffman 20X/0.55 magnification). NS, neurosphere

marker GFAP (Fig. 7). No differences were found in the qualitative localization of these antigens among cells from M1, M2, and M3.

### Discussion

This research demonstrates for the first time that FSH exerts regulatory actions on NSCs/NPCs derived in vitro from sheep OCCs, and on OCC-NS development. Relevant studies have unravelled the actions of different hormones on NSCs biology [21, 43] placing this issue at the

frontiers of endocrinology. In this research, two different culture strategies have allowed to investigate possible actions of FSH having yielded consistent and complementary results.

Regarding the identity of OCCs that generate NS, even though ovarian cortex needs to be fully characterized, OCCs suspension comprises a majority of stromal cells [44], surface epithelial cells (OSE pluripotent very small stem cells) [40], and possibly a residual number of granulosa cells entering the cell suspension after collagenase

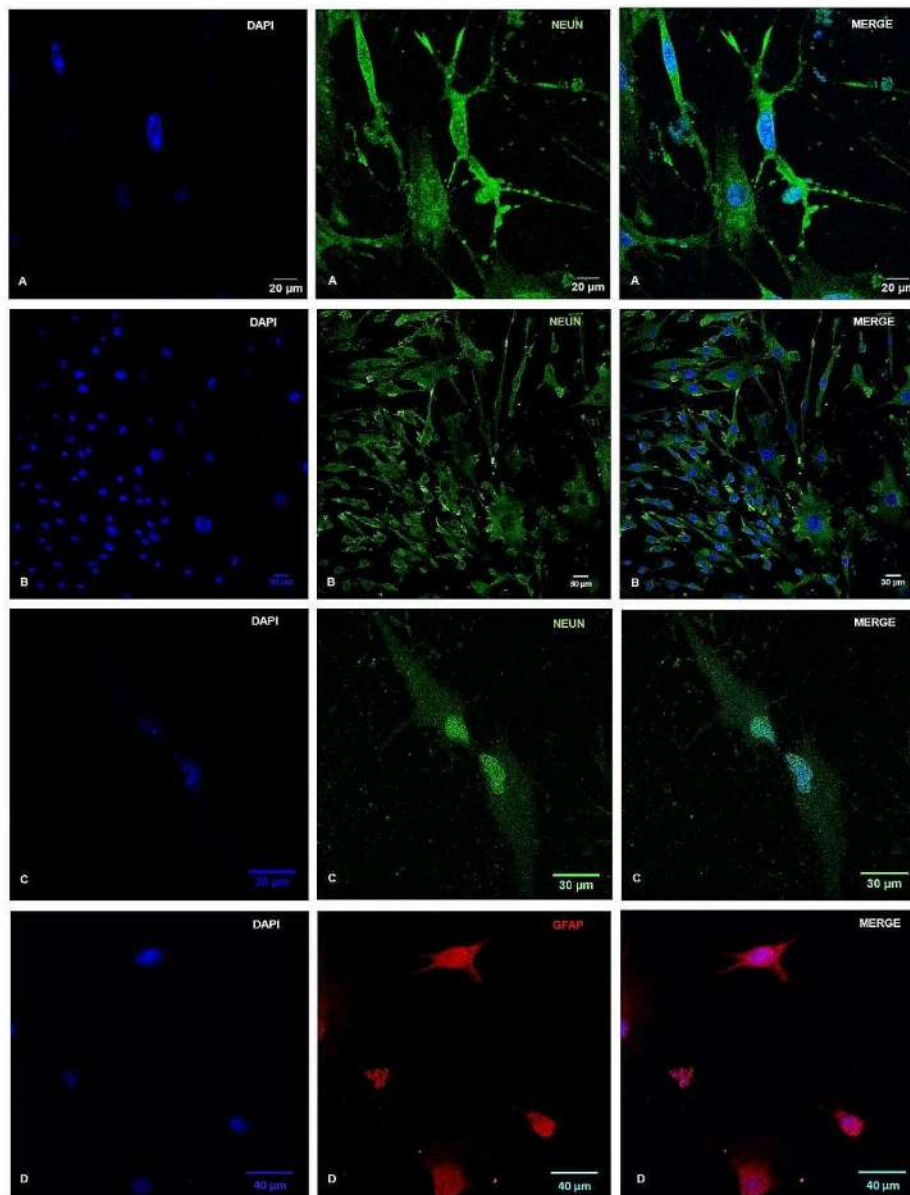


**Fig. 7** Photomicrographs showing immunofluorescent localization of NeuN (mature neurons; green, **A-C**), and GFAP (astrocytes; red, **D**) by confocal laser microscopy, on day 25 of culture for differentiation. NeuN was immunolocalized either in the cytoplasm only (**A, B**; HC PL APO CS2, 20X/0.75 dry), or in the cytoplasm and nucleus of a large proportion of cells (**C**; HC PL APO CS2 63X/1.40 oil). GFAP (**D**) was immunolocalized in many other cells in the same cultures. Nuclei were counterstained with DAPI (blue). DAPI, 4', 6-diamidino-2-phenylindole

tissue disaggregation, that most probably were eliminated from culture at the first medium replacement. In fact, earliest images taken between 24 and 72 h after the onset of culture, only showed two different cell types: elongated stromal cells and very small round epithelial cells (presumably OSE cells). Microphotographs evidenced that these two cell types established a paracrine interaction (Fig. 6A) that we hypothesize would cause neural induction of pluripotent OSE cells in a similar fashion as the system known as stromal cell derived inducing activity (SDIA). SDIA is an established co-culture system where stromal cells secrete neural inducing factors acting on pluripotent stem cells, to cause their neural specification into NSCs/NPCs [45].

In long-term cultures FSH caused an increase in NS diameters probably due to the stimulatory action of the hormone either on the expression of cell adhesion proteins that promote cell aggregation, or on its proliferative activity. In this regard, FSH upregulates the expression of the adhesion protein N-cadherin in tumour cells [46, 47] which would explain the rapid formation of NS, as the spheroids generated by all other stem cells [48]. On the other hand, FSH induces proliferation on VSELs at the OSE [49]. Since OCCs-NS derive from OSE cells, and express FSHR, larger NS diameters in FSH-group, likely result from a combination of these two mechanisms. Proliferative actions of FSH on OOC-NSCs/NPCs are supported by results during the NS assay. If the neurogenic capacity of stem cells relies in part on the size of NS generated in culture [10] then FSH may be considered a pro-neurogenic hormone.

An up-regulation of *Sox2* expression along with a down-regulation of *Oct4* and *Nanog* took place on day 10 of culture, as in previous studies [8, 9] which is a characteristic hallmark of neuroepithelial stem cell specification [50]. *Sox2* regulates pluripotency and sustains NSCs development [48] by repressing mesendoderm differentiation, to promote development of the neuroectodermal lineage [51].

FSH upregulated *Sox2* expression in NS on day 21 of culture. Despite no previous research has addressed hypothetical actions of FSH on *Sox2* expression, GnRH increased hypothalamic NSCs proliferation and *Sox2* expression in adult zebrafish [22]. This action might be mediated by FSH, since GnRH induces the release of this hormone from the pituitary gland. *Oct4* expression remained downregulated until day 15 of culture in both groups, and FSH increased it on day 21 over values of C-group. In this regard, FSH increases the expression of *Oct4* and *nestin* in brain and ovarian tumour cells improving sphere formation and self-renewal, by activating the ERK pathway [52, 53]. *Nanog* was downregulated during the whole culture period, which is coherent with

the neural specification of cells in culture since this transcript represses neuroectoderm differentiation [51].

Stem cell specification into NSCs was indicated by the predominant transcription and immunolocalization of *nestin*, *vimentin*, *p75NTR*, and *Pax6* [54] together with downregulation of *brachyury*, and *AFP*. FSH increased expression of *nestin* on days 15 and 21 in OCCs-NS. Accordingly, there was a time-dependent upward trend in the percentage of *nestin*-positive cells in FSH-group that increased on day 21 over values of C-group. This indicates that FSH might promote NSC self-renewal to maintain NSC pool in culture, in line with its actions on NSC proliferation and NS development, previously discussed. In fact, *nestin* participates in NS formation in the adult brain and is downregulated during NSC differentiation [55, 56]. *Nestin* was immunolocalised principally in the nucleus of cells placed at the outer sheet cover of the NS in both groups. Previous studies have demonstrated that nuclear localization of *nestin* is frequently found in proliferating cells in which *nestin* is transported into the nucleus [57] such as NPCs of vomeronasal organ during development [58], and NSCs/NPCs from the postnatal CNS [59]. The FSH-induced up-regulation of *nestin* and *Sox2* on day 21 of culture, along with its proliferative actions strongly supports that FSH has a relevant role in self-renewal of NSCs.

FSH increased the expression and immunolocalization of *Pax6* on days 15 and 21 of culture. Both the end of rise of *nestin* expression and the increase in transcription of *Pax6* between days 10 to 15 might be indicative of NSC transition to NPC ready to enter neural differentiation [60]. *Pax6* is a NPC marker that induces CNS-NSC proliferation, self-renewal and drives neurogenesis to generate basal progenitor cells and cortical neurons [61, 62]. Therefore, FSH might promote the transition from self-renewal to differentiation in these cells. *Sox2* and *Pax6* interrelationship must be highlighted here. Transcription of *Sox2* increased in both groups on day 10 in culture and decreased on day 15, when *Pax6* expression increased, which might be consistent with the transition of a significant proportion of cells from proliferation to differentiation on that day. The subsequent increase in *Sox2*, together with the high expression of *Pax6*, on day 21 might indicate that although a large part of the cells had left the NS and started to differentiate, other cells were beginning to proliferate in response to FSH.

Expression of *p75NTR* increased in both groups on day 10 of culture, and thereafter decreased as *Pax6* increased. Trk family of tyrosine kinases interact with p75NTR [63] to maintain stem cell potency, and this receptor is downregulated as cell differentiates [64–68] whereby p75NTR might be a key regulator of the maintenance of the undifferentiated state in stem cells [69]. Likewise, during the first 10 days of culture, cell expansion and

mitosis predominated simultaneously with a high expression of *p75NTR*. Later, as differentiation began to stand out, *p75NTR* expression decreased while *Pax6* transcription increased to reach maximum expression on day 21 of culture. Interestingly, previous research has demonstrated that *Pax6* down-regulates *p75NTR* in NPCs and that embryonic stem cells lacking *Pax6* generate GABAergic neurons overexpressing *p75NTR* with an elevated incidence of apoptosis [70]. FSH caused a reduction in *p75NTR*-positive NS-cells, supporting the view that it enhances NSC differentiation, as denoted by the simultaneous time-dependent upregulation of *Pax6*.

Lineage/developmental cluster analysis evidenced that NSC/NPC genes were the most expressed among all, highlighting an upregulation of *Pax6* from day 10 onwards. Interestingly, FSH increased the expression of pluripotency genes at the end of culture, in consistency with the upregulation of *Nanog* induced by FSH during CEP-2 of the NS assays, suggesting a possible action of this hormone in NSC reprogramming. The expression of NDC genes decreased as time in culture progressed, probably due to the inadequate composition of culture medium to sustain growth of neural-committed cells.

Results from NS assays demonstrated that OOC-NS cells displayed self-renewal capacity and proliferative activity that was stimulated by FSH in both CEP, as in previous research showing that FSH stimulated proliferation of VSELs and OSCs from sheep OSE after binding to FSHR3 [41]. This is consistent with the larger NS diameters found in FSH-group in comparison with C-group during long-term cultures, and by previous studies indicating that FSH stimulates self-renewal, expansion, and differentiation of VSELs into progenitors [38]. Self-renewal capacity was demonstrated by the spontaneous generation of NS during two consecutive CEP in all groups. In NS1, larger diameters were found in the presence of EGF and FGF2 (M1) and FSH (M3) in line with a greater proliferative activity of cells from these groups. EGF and FGF2 are neural inducing factors that stimulate NSCs proliferation [71] whereby they would promote the formation of NS in M1, used as positive control. Regarding the observed effects of FSH, it promotes self-renewal and proliferation of ovarian stem cells [40, 41] which would account for the larger development of NS in M3. Underlying mechanisms of the proliferative actions of FSH in these experiments, may involve an up-regulatory action of this hormone on *EGFR* transcription, as in OSE cells [72]. Some biomolecules synthesised by NSCs interact with *EGFR* to maintain self-renewal [73], like EGF and FGF2 constitutively secreted by ovarian somatic cells [74] and NSCs [75], that may act in an autocrine fashion to support their potency [76] and induce NSC proliferation instead of differentiation [77]. In fact, addition of EGF and FGF antagonists to culture medium is

frequently required to initiate NPC differentiation into mature neural cells [8, 12, 78].

Spontaneous formation of NS2 with NSCs/NPCs molecular identity confirmed self-renewal of NS-cells, as in previous studies [8]. Again, FSH (M3) increased NS cell proliferation over values of M2 and M1. The low proliferative activity in cells cultured in the presence of EGF and FGF2 (M1) is explained by the earlier confluence reached by these cells on the growth surface than cells from M2 and M3, as stated by image analysis. When cells become confluent in culture, intercellular contacts are established, and proliferative activity decreases [79] whereby on day 5 of M1-cells do not proliferate. In addition, NS1-cells, seeded at the onset of CEP-2 are NSCs/NPCs, unlike OCCs seeded at the onset of CEP-1 that may have minor proliferative potential, whereby NS1-cells would reach the confluence earlier than OCCs, particularly during exposure to EGF and FGF2 (M1).

The most expressed transcript in NS in both CEP was *nestin*, a characteristic marker of NSCs/NPCs [80] supporting the stability of cell identity in all groups. The lower *nestin* expression in NS1 from M3 compared with that of M2 might result from an inducing effect of FSH on the onset of NSC/NPC differentiation.

In NS2, FSH (M3) downregulated *Sox2* and *Oct4* and upregulated *Nanog* and *DCX*, when compared with M1 and M2 groups. Priming NS-cells with FSH during two consecutive CEP might have induced, in part of NS2-cells, a more immature phenotype, whereas some others might have progressed towards a neuronal cell fate, with increased expression of *DCX*, characteristic of neuronal precursors. This hypothetic action of FSH will be defined in future experiments.

Addition of EGF and FGF2 antagonists to differentiation culture medium triggered this process approximately 12 h later, as shown by image analysis with cell shape changes towards a neural or astrocytic morphology, whose incidence increased in cells exposed to FSH during two consecutive CEP. NS generation, evidenced as a less frequent event in this period, was accompanied by the formation of elongating projections connecting neighbouring NS, to generate a net of cellular bridges that was denser in NS from cells exposed to FSH during CEP. This is characteristic of NS during differentiation [81–83]. Microscopy observations demonstrated that cellular bridges were used by migrating cells with a high nucleus/cytoplasm ratio as a scaffold to move from one NS to another. Migrating cells showed morphological changes resembling those of neuroblasts as they move along the radial glia during neurogenesis [84]. Video time-lapse experiments will allow further investigation of these phenomena.

The identity of the differentiating cells was confirmed at the end of culture by localising specific antigens of

astrocytes, and mature neurons as in previous studies [8]. GFAP was immunolocalized in the cytoplasm of cells exhibiting morphological signs of astrocytic differentiation, and NeuN was expressed in a large proportion of cells differentiating on the growth surface, in which this antigen was predominantly immunolocalized in the cytoplasm, or in the cytoplasm and nucleus in a lesser proportion of cells. In this regard, it is well established that NeuN has several isoforms, and this antigen can be localized in both the nucleus and the cytoplasm [85–87]. The fact that priming with FSH during CEP upregulated DCX expression, suggests that this hormone might increase the density of neurons obtained during differentiation. This hypothesis will be addressed soon since it is of basic and applied interest.

## Conclusions

We can conclude that in OCCs-NS, FSH is a proneurogenic hormone that stimulates NSCs/NPCs proliferation, self-renewal, and increases the size of NS, upregulating *nestin*, *Sox2* and *Pax6*, and the percentages of NS-cells immunolocalizing the corresponding proteins in long-term cultures. NSCs/NPCs primed with FSH during culture for cell expansion exhibited increased expression of the neuron precursor transcript DCX. The proneurogenic actions of this hormone will be explored in future experiments to closely define whether it can be of potential use in basic and applied research in regenerative medicine.

## Abbreviations

AFP	Alpha-fetoprotein
BrdU	Bromodeoxyuridine
CEP	Cell expansion period
CNS	Central nervous system
CRH	Corticotropin-releasing hormone
DCX	Doublecortin
DMEM	Dulbecco's modified Eagle's medium
EGF	Epidermal growth factor
FGF2	Fibroblast growth factor 2
FSH	Follicle-stimulating hormone
FSHR	FSH receptor
GFAP	Glial fibrillary acidic protein
GnRH	Gonadotropin releasing hormone
NSPCs	Neural stem and progenitor cells
ITS	Insulin-transferrin-selenium
Nanog	Homeobox transcription factor
NS	Neurospheres
NSCs	Neural stem cells
NPCs	Neural progenitor cells
OCCs	Ovarian cortical cells
Oct4	Octamer binding transcription factor 4
Olig2	Oligodendrocyte specific transcript
Pax6	Paired box 6
p75NTR	Neurotrophin receptor p75
qRT-PCR	Quantitative Reverse Transcription Polymerase Chain Reaction
RQ	Relative quantification
SDIA	Stromal cell derived inducing activity
Sox2	Sex determining region Y-box 2
VSELs	Very small embryonic-like stem cells

## Supplementary Information

The online version contains supplementary material available at <https://doi.org/10.1186/s12917-024-04203-8>.

Supplementary Material 1

Supplementary Material 2

Supplementary Material 3

Supplementary Material 4

Supplementary Material 5

## Acknowledgements

The authors thank Pedro Aranda Espinosa for his technical support during sample processing for histology and immunohistochemistry; Ricardo García Mata for his work and collaboration on statistical analyses; Juan José Muñoz Oliveira, Alfonso Cortés Peña and Luis Alonso Colmenar for their expert technical help during fluorescence microscopy; Pilar Millán Pastor for providing technical equipment for enzyme immunoassay analyses; and Javier Cebrián for his logistic support to achieve the goals of this research project.

## Author contributions

A.G.G. participated in the experimental designs, cell culture, morphometric evaluation, neurosphere assays, statistical analyses and manuscript redaction; B.S.M. contributed to the experimental designs and immunohistochemical analyses; C.R.S. participated in the experimental designs and immunofluorescent localization of antigens; M.F.G. contributed to the neurosphere assays and statistical analyses; F.L.Q. participated in the immunofluorescent localization of antigens and funding search; S.O.A. and R.R.R. participated in the oligonucleotide design and qRT-PCR analyses; M.F.R. contributed to the cell isolation and culture, and morphometric evaluation; R.A.P.G. participated in the experimental designs, cell culture, morphometric evaluation, neurosphere assays, statistical analyses, manuscript redaction and funding search. All authors participated in the critical manuscript review, read and approved the final manuscript.

## Funding

This work was financed by National Funds (FCT/MCTES, Fundação para a Ciência e a Tecnologia and Ministério da Ciência, Tecnologia e Ensino Superior) under the project UIDB/00211/2020. Authors want also thanks the support received by the Ministerio de Economía y Competitividad, Gobierno de España (research grant AGL/2008–03227), by Universidad Complutense de Madrid, Programa de Creación y Consolidación de Grupos de Investigación (research group UCM-920380), UCM-Santander Research Grants (research grant PR41/17-21020) and by project UIDB/04033/2020, from FCT/MCTES.

## Data availability

Data are available from the corresponding author upon reasonable request.

## Declarations

### Ethics approval and consent to participate

Not applicable. Biological material from slaughterhouse animals under veterinary inspection was used. Under such circumstances, no formal review by an Institutional Animal Care and Use Committee was required.

### Consent for publication

Not applicable.

### Competing interests

The authors declare no competing interests.

### Author details

<sup>1</sup>Department of Physiology, School of Veterinary Medicine, Complutense University of Madrid, Avda. Puerta de Hierro SN, Madrid 28040, Spain

<sup>2</sup>Department of Animal Medicine and Surgery, School of Veterinary Medicine, Complutense University of Madrid, Madrid 28040, Spain

<sup>3</sup>Department of Anatomy and Embriology, School of Veterinary Medicine, University Complutense of Madrid, Madrid 28040, Spain

<sup>4</sup>Department of Molecular Neuropathology, Centro de Biología Molecular “Severo Ochoa” (CBMSO), Spanish Research Council (CSIC)-Universidad Autónoma de Madrid, Madrid 28049, Spain

<sup>5</sup>Department of Molecular Biology, Faculty of Sciences, Universidad Autónoma de Madrid, Madrid 28049, Spain

<sup>6</sup>Centre for the Study of Animal Science, CECA-ICETA, University of Porto, Porto, Portugal

<sup>7</sup>Animal and Veterinary Research Centre (CECAV), University of Trás-os-Montes and Alto Douro, Quinta dos Prados, Vila Real 5000-801, Portugal

<sup>8</sup>Genomic Unit Cantoblanco, Fundación Parque Científico de Madrid. C/ Faraday 7, Madrid 28049, Spain

Received: 26 January 2024 / Accepted: 23 July 2024

Published online: 20 August 2024

## References

- Zakrzewski W, Dobrzyński M, Szymonowicz M, Ryback Z. Stem cells: past, present, and future. *Stem Cell Res Ther*. 2019;10(1):68.
- Rajabzadeh N, Fathi E, Farahzadi R. Stem cell-based regenerative medicine. *Stem Cell Investig*. 2019;6:19.
- Azari H, Reynolds BA. In vitro models for neurogenesis. *Cold Spring Harb Perspect Biol*. 2016;8(6):a021279.
- La Rosa C, Bonfanti L. Searching for alternatives to brain regeneration. *Neural Regen Res*. 2021;16(11):2198–200.
- Amoh Y, Mii S, Aki R, Hamada Y, Kawahara K, Hoffman RM, et al. Multipotent nestin expressing stem cells capable of forming neurons are located in the upper, middle and lower part of the vibrissa hair follicle. *Cell Cycle*. 2012;11(18):3513–17.
- Romero-Ramos M, Vourc'h P, Young H, Lucas PA, Wu Y, Chivatakarn O, et al. Neuronal differentiation of stem cells isolated from adult muscle. *J Neurosci Res*. 2002;69(6):894–907.
- Solis-Castro OO, Boissonade FM, Rivolta MN. Establishment and neural differentiation of neural crest derived stem cells from human dental pulp in serum-free conditions. *Stem Cells Transl Med*. 2020;9(11):1462–76.
- Sánchez-Maldonado B, Galicia ML, Rojo Salvador C, González-Gil A, Flor-García M, Picazo RA. Spheroids spontaneously generated in vitro from sheep ovarian cortical cells contain integrating cells that exhibit hallmarks of neural stem/progenitor cells. *Stem Cells Dev*. 2018;27(22):1557–76.
- Rojo Salvador C, Galicia ML, Sánchez-Maldonado B, González-Gil A, Picazo RA. Morphological and ultrastructural characterization of neurospheres spontaneously generated in the culture from sheep ovarian cortical cells. *Anat Rec (Hoboken)*. 2022;305(9):2265–80.
- Ladiwala U, Basu H, Mathur D. Assembling neurospheres: dynamics of neural progenitor/stem cell aggregation probed using an optical trap. *PLoS ONE*. 2012;7(6):e38613.
- Tsai AC, Liu Y, Yuan X, Ma T. Compaction, fusion, and functional activation of three-dimensional human mesenchymal stem cell aggregate. *Tissue Eng Part A*. 2015;21(9–10):1705–19.
- Nieto-Estévez V, Pignatelli J, Araújo-Bravo MJ, Hurtado-Chong A, Vicario-Abelón C. A global transcriptome analysis reveals molecular hallmarks of neural stem cell death, survival, and differentiation in response to partial FGF-2 and EGF deprivation. *PLoS ONE*. 2013;8(1):e53594.
- Yang CC, Graves HK, Moya IM, Tao C, Hamaratoglu F, Gladden AB, et al. Differential regulation of the Hippo pathway by adherens junctions and apical-basal cell polarity modules. *PNAS*. 2015;112:1785–90.
- Soares R, Ribeiro FF, Lourenço DM, Rodrigues RS, Moreira JB, Sebastião AM, et al. The neurosphere assay: an effective in vitro technique to study neural stem cells. *Neural Regen Res*. 2021;16(11):2229–31.
- Fritsche E, Grandjean P, Crofton KM, Aschner M, Goldberg A, Heinonen T, et al. Consensus statement on the need for innovation, transition and implementation of developmental neurotoxicity (DNT) testing for regulatory purposes. *Toxicol Appl Pharmacol*. 2018;354:3–6.
- Carvalho IM, Coelho PB, Costa PC, Marques CS, Oliveira RS, Ferreira DC. Current neurogenic and neuroprotective strategies to prevent and treat neurodegenerative and neuropsychiatric disorders. *Neuromolecular Med*. 2015;17(4):404–22.
- Marsh SE, Blurton-Jones M. Neural stem cell therapy for neurodegenerative disorders: the role of neurotrophic support. *Neurochem Int*. 2017;106:94–100.
- Jorgensen C, Wang Z. Hormonal regulation of mammalian adult neurogenesis: a multifaceted mechanism. *Biomolecules*. 2020;10(8):1151.
- Mahmoud R, Wainwright SR, Galea LA. Sex hormones and adult hippocampal neurogenesis: regulation, implications, and potential mechanisms. *Front Neuroendocrinol*. 2016;41:129–52.
- Lévy F, Batailler M, Meurisse M, Keller M, Cornilleau F, Moussu C, et al. Differential effects of oxytocin on olfactory, hippocampal and hypothalamic neurogenesis in adult sheep. *Neurosci Lett*. 2019;713:134520.
- Velasco I. Stem cells with neurogenic potential and steroid hormones. *Curr Top Med Chem*. 2011;11(13):1684–93.
- Ceriani R, Whitlock KE. Gonadotropin releasing hormone (GnRH) triggers neurogenesis in the hypothalamus of adult zebrafish. *Int J Mol Sci*. 2021;22(1):5926.
- Wickramasuriya N, Hawkins R, Atwood C, Butler T. The roles of GnRH in the human central nervous system. *Horm Behav*. 2022;145:105230.
- Hamson DK, Wainwright SR, Taylor JR, Jones BA, Watson NV, Galea LA. Androgens increase survival of adult-born neurons in the dentate gyrus by an androgen receptor-dependent mechanism in male rats. *Endocrinology*. 2013;154(9):3294–304.
- Shohayeb B, Diab M, Ahmed M, Ng DCH. Factors that influence adult neurogenesis as potential therapy. *Transl Neurodegener*. 2018;7:4.
- Spritzer MD, Roy EA. Testosterone and adult neurogenesis. *Biomolecules*. 2020;10(2):225.
- Kraemer RR, Kraemer BR. The effects of peripheral hormone responses to exercise on adult hippocampal neurogenesis. *Front Endocrinol (Lausanne)*. 2023;14:1202349.
- Triviño-Paredes J, Patten AR, Gil-Mohapel J, Christie BR. The effects of hormones and physical exercise on hippocampal structural plasticity. *Front Neuroendocrinol*. 2016;41:23–43.
- Wang JM, Liu L, Brinton RD. Estradiol-17beta-induced human neural progenitor cell proliferation is mediated by an estrogen receptor beta-phosphorylated extracellularly regulated kinase pathway. *Endocrinology*. 2008;149(1):208–18.
- Scharfman HE, MacLusky NJ. Estrogen and brain-derived neurotrophic factor (BDNF) in hippocampus: complexity of steroid hormone-growth factor interactions in the adult CNS. *Front Neuroendocrinol*. 2006;27(4):415–35.
- Galea LA. Gonadal hormone modulation of neurogenesis in the dentate gyrus of adult male and female rodents. *Brain Res Rev*. 2008;57(2):332–41.
- Garza JC, Guo M, Zhang W, Lu XY. Leptin increases adult hippocampal neurogenesis in vivo and in vitro. *J Biol Chem*. 2008;283(26):18238–47.
- Remaud S, Gothié JD, Morvan-Dubois G, Demeneix BA. Thyroid hormone signaling and adult neurogenesis in mammals. *Front Endocrinol (Lausanne)*. 2014;5:62.
- Kim C, Kim S, Park S. Neurogenic effects of Ghrelin on the Hippocampus. *Int J Mol Sci*. 2017;18(3):588.
- Koutmani Y, Gampierakis IA, Polissidis A, Ximerakis M, Koutsoudaki PN, Polyzos A, Agrogiannis G, Karaliota S, Thomaïdou D, Rubín LL, Politis PK, Karalis KP. CRH promotes the neurogenic activity of neural stem cells in the adult hippocampus. *Cell Rep*. 2019;29(4):932–e457.
- Xiong J, Kang SS, Wang Z, Liu X, Kuo TC, Korkmaz F, et al. FSH blockade improves cognition in mice with Alzheimer's disease. *Nature*. 2022;603(7901):470–6.
- Llorente V, Velarde P, Desco M, Gómez-Gaviró MV. Current understanding of the neural stem cell niches. *Cells*. 2022;11(19):3002.
- Bhartiya D, Patel H, Kaushik A, Singh P, Sharma D. Endogenous, tissue-resident stem/progenitor cells in gonads and bone marrow express FSHR and respond to FSH via FSHR-3. *J Ovarian Res*. 2021;14(1):145.
- Patel H, Bhartiya D, Parte S. Further characterization of adult sheep ovarian stem cells and their involvement in neo-oogenesis and follicle assembly. *J Ovarian Res*. 2018;11(1):3.
- Parte S, Bhartiya D, Manjramkar DD, Chauhan A, Joshi A. Stimulation of ovarian stem cells by follicle stimulating hormone and basic fibroblast growth factor during cortical tissue culture. *J Ovarian Res*. 2013;6(1):20.
- Patel H, Bhartiya D, Parte S, Gunjal P, Yedurkar S, Bhatt M. Follicle stimulating hormone modulates ovarian stem cells through alternately spliced receptor variant FSH-R3. *J Ovarian Res*. 2013;6:52.
- Azari H, Rahman M, Shariffar S, Reynolds BA. Isolation and expansion of the adult mouse neural stem cells using the neurosphere assay. *J Vis Exp*. 2010;45:2393.
- Bramble MS, Vashist N, Vilain E. Sex steroid hormone modulation of neural stem cells: a critical review. *Biol Sex Differ*. 2019;10(1):28.
- Gong SP, Lee JH, Lim JM. Derivation of histocompatible stem cells from ovarian tissue. *J Reprod Dev*. 2010;56(5):481–94.

45. Vazin T, Chen J, Lee CT, Amable R, Freed WJ. Assessment of stromal-derived inducing activity in the generation of dopaminergic neurons from human embryonic stem cells. *Stem Cells*. 2008;26(6):1517–25.
46. Kolnes AJ, Øystese KAB, Olarescu NC, Ringstad G, Berg-Johnsen J, Casar-Borota O, et al. FSH levels are related to e-cadherin expression and subcellular location in nonfunctioning pituitary tumors. *J Clin Endocrinol Metab*. 2020;105(8):2587–94.
47. Sheng S, Liu W, Xue Y, Pan Z, Zhao L, Wang F, et al. Follicle-stimulating hormone promotes the development of endometrial cancer in vitro and in vivo. *Int J Environ Res Public Health*. 2022;19(22):15344.
48. Cesarz Z, Tamama K. Spheroid culture of mesenchymal stem cells. *Stem Cells Int*. 2016;2016:9176357.
49. Bhartiya D, Singh J. FSH-FSHR3-stem cells in ovary surface epithelium: basis for adult ovarian biology, failure, ageing, and cancer. *Reproduction*. 2015;149(1):R35–48.
50. Zhang S, Cui W. Sox2, a key factor in the regulation of pluripotency and neural differentiation. *World J Stem Cells*. 2014;6(3):305–11.
51. Wang Z, Oron E, Nelson B, Razi S, Ivanova N. Distinct lineage specification roles for NANOG, OCT4, and SOX2 in human embryonic stem cells. *Cell Stem Cell*. 2012;10(4):440–54.
52. Liu L, Zhang J, Fang C, Zhang Z, Feng Y, Xi X. OCT4 mediates FSH-induced epithelial-mesenchymal transition and invasion through the ERK1/2 signaling pathway in epithelial ovarian cancer. *Biochem Biophys Res Commun*. 2015;461:525–32.
53. Wang F, Wang AY, Chesnelong C, Yang Y, Nabbi A, Thalappilly S, et al. ING5 activity in self-renewal of glioblastoma stem cells via calcium and follicle stimulating hormone pathways. *Oncogene*. 2018;37(3):286–301.
54. Zhang J, Jiao J. Molecular biomarkers for embryonic and adult neural stem cell and neurogenesis. *Biomed Res Int*. 2015;2015:727542.
55. Mignone JL, Kukekov V, Chiang AS, Steindler D, Enikolopov G. Neural stem and progenitor cells in nestin-GFP transgenic mice. *J Comp Neurol*. 2004;469(3):311–24.
56. Bernal A, Arranz L. Nestin-expressing progenitor cells: function, identity and therapeutic implications. *Cell Mol Life Sci*. 2018;75(12):2177–95.
57. Sahlgren CM, Mikhailov A, Hellman J, Chou YH, Lendahl U, Goldman RD, Eriksson JE. Mitotic reorganization of the intermediate filament protein nestin involves phosphorylation by cdc2 kinase. *J Biol Chem*. 2001;276(19):16456–63.
58. Merigo F, Mucignat-Caretta C, Zancanaro C. Timing of neuronal intermediate filament proteins expression in the mouse vomeronasal organ during pre- and postnatal development. An immunohistochemical study. *Chem Senses*. 2005;30:707–17.
59. Namiki Namiki J, Suzuki S, Masuda T, Ishihama Y, Okano H. Nestin protein is phosphorylated in adult neural stem/progenitor cells and not endothelial progenitor cells. *Stem Cells Int*. 2012;2012:430138.
60. Sakurai K, Osumi N. The neurogenesis controlling factor, PAX6, inhibits proliferation and promotes maturation in murine astrocytes. *J Neurosci*. 2008;28:4604–12.
61. Sansom SN, Griffiths DS, Faedo A, Kleinjan DJ, Ruan Y, Smith J, et al. The level of the transcription factor Pax6 is essential for controlling the balance between neural stem cell self-renewal and neurogenesis. *PLoS Genet*. 2009;5(6):e1000511.
62. Hack MA, Sugimori M, Lundberg C, Nakafuku M, Götz M. Regionalization and fate specification in neurospheres: the role of Olig2 and Pax6. *Mol Cell Neurosci*. 2004;25(4):664–78.
63. Roux PP, Barker PA. Neurotrophin signalling through the p75 neurotrophin receptor. *Prog Neurobiol*. 2002;67(3):203–33.
64. Lambiasi A, Aloe L, Mantelli F, Sacchetti M, Perrella E, Bianchi P, et al. Capsaicin-induced corneal sensory denervation and healing impairment are reversed by NGF treatment. *Invest Ophthalmol Vis Sci*. 2012;53(13):8280–7.
65. Schuldiner M, Yanuka O, Itskovitz-Eldor J, Melton DA, Benvenisty N. Effects of eight growth factors on the differentiation of cells derived from human embryonic stem cells. *Proc Natl Acad Sci U S A*. 2000;97(21):11307–12.
66. Bibel M, Richter J, Schrenk K, Tucker KL, Staiger V, Korte M, et al. Differentiation of mouse embryonic stem cells into a defined neuronal lineage. *Nat Neurosci*. 2004;7(9):1003–9.
67. Chalazonitis A. Neurotrophin-3 in the development of the enteric nervous system. *Prog Brain Res*. 2004;146:243–63.
68. Quirici N, Soligo D, Bossolasco P, Servida F, Lumini C, Deliliers GL. Isolation of bone marrow mesenchymal stem cells by anti-nerve growth factor receptor antibodies. *Exp Hematol*. 2002;30(7):783–91.
69. Thomson TM, Rettig WJ, Chesa PG, Green SH, Mena AC, Old LJ. Expression of human nerve growth factor receptor on cells derived from all three germ layers. *Exp Cell Res*. 1988;174(2):533–9.
70. Nikolettou V, Plachta N, Allen ND, Pinto L, Götz M, Barde YA. Neurotrophin receptor-mediated death of misspecified neurons generated from embryonic stem cells lacking Pax6. *Cell Stem Cell*. 2007;1(5):529–40.
71. Bazán E, Alonso FJM, Redondo C, López-Toledano MA, Alfaro JM, Reimers D, et al. In vitro and in vivo characterization of neural stem cells. *Histol Histopathol*. 2004;19(4):1261–75.
72. Choi JH, Choi KC, Auersperg N, Leung PC. Gonadotropins upregulate the epidermal growth factor receptor through activation of mitogen-activated protein kinases and phosphatidylinositol-3-kinase in human ovarian surface epithelial cells. *Endocr Relat Cancer*. 2005;12(2):407–21.
73. Wang J, Yu RK. Interaction of ganglioside GD3 with an EGF receptor sustains the self-renewal ability of mouse neural stem cells in vitro. *Proc Natl Acad Sci U S A*. 2013;110(47):19137–42.
74. Berisha B, Schams D, Kosmann M, Amselgruber W, Einspanier R. Expression and localisation of vascular endothelial growth factor and basic fibroblast growth factor during the final growth of bovine ovarian follicles. *J Endocrinol*. 2000;167(3):371–82.
75. Lu P, Jones LL, Snyder EY, Tuszynski MH. Neural stem cells constitutively secrete neurotrophic factors and promote extensive host axonal growth after spinal cord injury. *Exp Neurol*. 2003;181(2):115–29.
76. Mori H, Ninomiya K, Kino-oka M, Shofuda T, Islam MO, Yamasaki M, et al. Effect of neurosphere size on the growth rate of human neural stem/progenitor cells. *J Neurosci Res*. 2006;84(8):1682–91.
77. Schomberg DW, May JV, Mondschein JS. Interactions between hormones and growth factors in the regulation of granulosa cell differentiation in vitro. *J Steroid Biochem*. 1983;19(1A):291–5.
78. Lee JH, Shaker MR, Lee E, Lee B, Sun W. NeuroCore formation during differentiation of neurospheres of mouse embryonic neural stem cells. *Stem Cell Res*. 2020;43:101691.
79. Balint R, Richardson SM, Cartmell SH. Low-density subculture: a technical note on the importance of avoiding cell-to-cell contact during mesenchymal stromal cell expansion. *J Tissue Eng Regen Med*. 2015;9(10):1200–03.
80. Park D, Xiang AP, Mao FF, Zhang L, Di CG, Liu XM, et al. Nestin is required for the proper self-renewal of neural stem cells. *Stem Cells*. 2010;28(12):2162–71.
81. Jeong GS, Chang JY, Park JS, Lee SA, Park D, Woo J, et al. Networked neural spheroid by neuro-bundle mimicking nervous system created by topology effect. *Mol Brain*. 2015;8:17.
82. Crepaldi CR, Fonseca Merighe GK, Laure HJ, Rosa JC, Meirelles FV, Cerqueira César M. Isolation and culture of neurons and neurospheres from chicken brain cortex. *Pesq Vet Bras* [online]. 2013;33(1):45–50.
83. Jorfi M, D'Avanzo C, Tanzi RE, Kim DY, Irimia D. Human neurospheroid arrays for in vitro studies of Alzheimer's disease. *Sci Rep*. 2018;8(1):2450.
84. Taverna E, Götz M, Huttner WB. The cell biology of neurogenesis: toward an understanding of the development and evolution of the neocortex. *Annu Rev Cell Dev Biol*. 2014;30:465–502.
85. Lind D, Franken S, Kappler J, Jankowski J, Schilling K. Characterization of the neuronal marker NeuN as a multiply phosphorylated antigen with discrete subcellular localization. *J Neurosci Res*. 2005;79(3):295–302.
86. Dredge BK, Jensen KB. NeuN/Rbfox3 nuclear and cytoplasmic isoforms differentially regulate alternative splicing and nonsense-mediated decay of Rbfox2. *PLoS ONE*. 2011;6(6):e21585.
87. Anderson MB, Das S, Miller KE. Subcellular localization of neuronal nuclei (NeuN) antigen in size and calcitonin gene-related peptide (CGRP) populations of dorsal root ganglion (DRG) neurons during acute peripheral inflammation. *Neurosci Lett*. 2021;760:135974.

## Publisher's Note

Springer Nature remains neutral with regard to jurisdictional claims in published maps and institutional affiliations.